A Global Potential Energy Surface Describing the N(2 D) + H 2 O Reaction and a Quasiclassical Trajectory Study of the Reaction to NH + OH

ARTICLE *in* THE JOURNAL OF PHYSICAL CHEMISTRY A · DECEMBER 2013

Impact Factor: 2.69 · DOI: 10.1021/jp410935k · Source: PubMed

2 AUTHORS:

Zahra Homayoon
Emory University
18 PUBLICATIONS **98** CITATIONS
SEE PROFILE

Joel M Bowman
Emory University
541 PUBLICATIONS **15,063** CITATIONS
SEE PROFILE

THE JOURNAL OF PHYSICAL CHEMISTRY A

Article

pubs.acs.org/JPCA

A Global Potential Energy Surface Describing the N(^{2}D) + H_2O Reaction and a Quasiclassical Trajectory Study of the Reaction to NH + OH

Zahra Homayoon* and Joel M. Bowman*

Department of Chemistry and Cherry L. Emerson Center for Scientific Computation, Emory University, Atlanta, Georgia 30322, United States

ABSTRACT: We report a global potential energy surface (PES) for the N(^{2}D) + H_2O reaction based on fitting roughly 312 000 UCCSD(T)-F12/aug-cc-pVTZ electronic energies. The surface is a linear least-squares fit using a permutationally invariant basis with Morse-type variables. Quasiclassical trajectory calculations of the N(^{2}D) + H_2O(D_2O) reaction with focus on the NH(D) + OH(D) exit channel are performed. An analysis of the internal-state distributions shows that the NH(D) fragment has more internal energy, both rotational and vibrational than the OH(D) fragment, in good agreement with experiment. This difference is traced to nonstatistical dynamics.

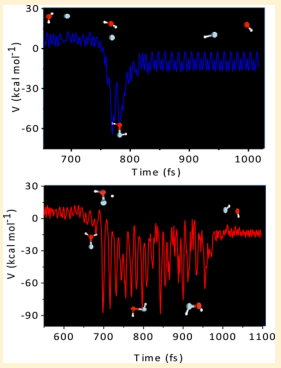

INTRODUCTION

The reaction of N(^{2}D) with H_2O is an important chemical processes in the atmosphere of the earth and combustion of nitrogen-containing fuels.[1] There are five possible exit channels for this reaction:

$$N(^2D) + H_2O(^1A_1) \rightarrow NH(X^3\Sigma^-) + OH(X^2\Pi) \quad (R1)$$

$$\rightarrow HNO(1A'') + H \quad (R2)$$

$$\rightarrow HON(^3A'') + H \quad (R3)$$

$$\rightarrow NO(^2\Pi) + H_2(^1\Sigma_g) \quad (R4)$$

$$\rightarrow NH_2(^2B_1) + O(^3P) \quad (R5)$$

The exothermicity of these five channels from theoretical calculations and thermodynamical data are given in Table 1 along with the corresponding discussion. The importance of this system has also led to several studies experimentally on the reactions NO + H_2,[2] HNO + H,[3] and O + NH_2[4−6,9,10] and the title reaction.[7,8]

Early studies of the N(^{2}D) + H_2O (D_2O) reaction were done by Umemoto et al.[7] in 1999. Ground-state NH(D) and OH(D) radicals using laser induced fluorescence as well as H(D) atoms were detected as products. They reported the production of NH + OH as one of the main reaction channels. Their experiment revealed nonstatistical internal-state distributions of both NH and OH. However, NH was found more internally excited than OH, both rotationally and vibrationally. They also reported the H atom as the H + HNO(^{1}A′) product channel, reaction R2. The average energy released into the translational mode in these products was reported as 65 kJ mol^{-1} corresponding to 45% of the available energy for the products.

In 2001 the dynamics of the N(^{2}D) + H_2O reaction was investigated by using the crossed molecular beam scattering method with mass spectrometric detection of products by Casavecchia et al.[8] The channels that they could conveniently investigate with their technique were those of H-displacement, leading to the two possible isomers HNO and HON and that of H_2-elimination, leading to the formation of NO. Their experiments showed the N/H exchange channel via two competing pathways leading to HNO + H and HON + H, whereas formation of NO + H_2 is negligible.

Theoretically some of the relevant channels of the N(^{2}D) + H_2O reaction had been studied in 1998 by Sumathi et al.[11] The study contains the mechanisms of the reactions occurring on the lowest doublet potential energy surface of the [H_2NO] system at the CCSD(T)/6-311++G(3df,3pd)//CCSD(T)/6-311++G (d,p) level of theory. The paper reports H_2NO, HNOH, and H_2ON intermediates and includes the H_2 + NO, NH_2 + O, NH + OH, and H + HNO as entrance channels.

In 1999, ab initio molecular orbital calculations were carried out for the N(^{2}D) + H_2O reaction by Kurosaki et al.[12] They examined the reaction pathways at the PMP4(full,SDTQ)/cc-pVTZ//MP2(full)/cc-pVTZ level of theory. NH($^3\Sigma$) + OH($^2\Pi$), HNO(^{1}A′) + H, and NO($^2\Pi$) + H_2 were predicted as main channels. On the basis of these calculations, production of mentioned fragments takes place through formation of H_2ON, *cis*-HONH, *trans*-HONH, and H_2NO intermediates. It

Received: November 6, 2013
Revised: December 19, 2013
Published: December 30, 2013

   dx.doi.org/10.1021/jp410935k | *J. Phys. Chem. A* 2014, 118, 545−553

Table 1. Stationary Point Energies (kcal mol^{-1}) of the Fitted Potential Energy Surface (PES), UCCSD(T)-F12/aug-cc-pVTZ and UCCSD(T)-F12/aug-cc-pVQZ, and Zero Point Energies[a]

	CCSD(T)-F12/aug-cc-pVTZ	CCSD(T)-F12/aug-cc-pVQZ	PES	ZPE[b]	exp[d]
$N(^2D) + H_2O$	0.0	0.0	0.0	13.61	
HNO + H	−32.30 (−37.13)	−32.75 (−37.58)	−32.61 (−37.44)	8.78	−40.88
HON + H	−7.19 (−11.96)	−7.25 (−12.02)	−7.32 (−12.09)	8.84	
NH+ OH	−18.0 (−21.24)	−17.97 (−21.21)	−17.58 (−20.82)	10.37	−17.38
NO + H_2	−88.47 (−91.07)	−89.12 (−91.71)	−89.00 (−91.60)	11.01	−95.18
O + H_2N	−10.33 (−11.65)	−10.36 (−11.68)	−9.96 (−11.28)	12.29	−11.68
H_2ON	−20.21	−20.65	−19.42	17.10	
cis-HNOH	−89.01	−89.34	−88.75	16.79	
trans-HNOH	−94.53	−94.86	−94.9	17.32	
H_2NO ($^2B_1$)	−101.43	−101.68	−101.21	16.99	
TS1	−14.05	−14.36	−14.75	14.74	
TS2	−79.94	−80.28	−79.51	15.52	
TS3	−47.36	−47.65	−47.25	14.72	
TS4	−31.83	−32.21	−32.71	11.95	
TS5[c]	−33.42	−32.98	−32.72	10.60	
TS6	−25.55	−27.00	−25.78	10.86	
TS7	4.47	4.31	3.90	11.80	

[a]ZPE corrected values are given in parentheses. [b]ZPE energies are calculated at MP2/6-311+G(d,p). [c]Calculated at UCCSD(T)/aug-cc-pVTZ and UCCSD(T)/aug-cc-pVQZ levels of theory. [d]Reference 21.

was found that a nonadiabatic process significantly contributes to the $NO(^2\Pi) + H_2$ channel via dissociation of H_2NO intermediate.

One disagreement in the calculations of refs 11 and 12 is the saddle point for the dissociation of ground state of H_2NO to $NO + H_2$. The barrier for the dissociation of H_2NO to $NO + H_2$ was shown as 62.1 and 90 kcal mol^{-1}, in refs 11 and 12, respectively. In 2000 Kurosaki et al.[13] reexamined this pathway at the FOCI/cc-pVTZ level of theory for two electronic states and obtained a barrier in close agreement with the value calculated in ref 11.

The reported investigations of stationary points of potential energy surface[11,12] show a very complicated mechanism for the title reaction. Association of the $N(^2D) + H_2O$ reactants produce several intermediates. The available energy for three intermediates, *cis*-HONH, *trans*-HONH, and H_2NO, is ∼100 kcal mol^{-1}. Vibrationally excited intermediates could dissociate into five exit channels (R1)−(R5). All channels are accessible at very low collision energies of the reactants and for some products there is more than one pathway. Although experimentally energy partitioning of some products has been investigated, dynamical calculations based on a reliable potential energy surface that could reveal the details of mechanism of the reactions have not been studied.

The complicated mechanism of the $N(^2D) + H_2O$ reaction[11,12] and limited theoretical studies motivated us to develop a global potential energy surface. The main goal of the present paper is to report the first full-dimensional global potential energy surface for the reaction at a high level of theory including all reaction channels given above. This is a challenging system because of the number of exit pathways and the regions of open-shell character. In the present paper a global potential energy surface for the $N(^2D) + H_2O$ reaction is reported on the basis of a data set at UCCSD(T)-F12/aug-cc-pVTZ level of theory, with details given below.

The paper is organized as follows. In the next section we give details of the electronic calculations and the construction of the global PES. Then properties of the PES are given along with tests of the PES both representing the electronic energies and structures of stationary points. Minimum energy paths for isomerization of intermediates and their dissociation to fragments are also reported from direct ab initio calculations and their comparison with the fitted PES. The last section describes quasiclassical trajectory calculations (QCT) for the $N(^2D) + H_2O$ and D_2O reactions with a focus on details of energy distribution of products of reaction R1.

CALCULATION DETAILS

The calculations started with a reexamination of the reported reaction paths[11,12] at a high level of theory. The ab initio calculations were carried out using MOLPRO 2008,[14] GAUSSIAN 2009,[15] and MOLCAS[16] programs. Geometry optimizations were done initially at the UMP2/6-311+G(d,p) level and then reoptimized at the UCCSD(T)/6-311+G(d,p) level of theory. Stationary points were characterized by harmonic vibrational frequency analyses at the UMP2/6-311+G(d,p) level. Reaction paths were established by intrinsic reaction coordinate (IRC) calculations. Finally, single-point calculations of the optimized geometries were computed using the UCCSD(T)-F12b level of theory using aug-cc-pVTZ and aug-cc-pVQZ basis sets to obtain improved estimate for their relative energies. Multireference regions of reaction paths were treated using MS-CASPT2(11e,11o)/cc-pVTZ level of theory for two electronic states, as will be discussed below. The zero-point energies were derived from harmonic vibrational energies at the UMP2/6-311+G(d,p) level.

The next section describes the details of construction of potential energy surface of the title reaction.

CONSTRUCTION OF POTENTIAL ENERGY SURFACE

The construction of a global PES begins by considering the regions of configuration space that the PES should describe at the reactants' energy of interest. In the $N(^2D) + H_2O$ reaction the first regions describe the initial steps of $N(^2D)$ and H_2O association. Association of the reactants forms the H_2ON intermediate, followed by three isomerization pathways to make *trans*-HONH, *cis*-HONH, and H_2NO intermediates. Even with

dx.doi.org/10.1021/jp410935k | J. Phys. Chem. A 2014, 118, 545−553

very low collision energy, the available energy for the intermediates is ~100 kcal mol^{-1}. So the data set needs enough data to describe the vibrationally excited intermediate up to this level. HNO + H, HON + H, NH + OH, H_2 + NO, and O + NH_2 are the products of dissociation of intermediates. Details of the all pathways are given with explanation of properties of fitted PES in the next section.

We sampled the reaction pathways with direct-dynamics calculations at the UB3LYP/6-311+G(d,p) level of theory. Roughly 300 trajectories were run, initiated at intermediates and saddle points at different energies to gather a variety of data. Several methods and basis sets were examined for the stationary points and finally we selected the UCCSD(T)-F12/aug-cc-pVTZ level of theory to generate the electronic energies for the fitting database. Collected data from direct dynamics calculations were recalculated at this level of theory.

Fragment energies were obtained as well, using UCCSD(T)-F12/aug-cc-pVTZ calculations. For products we added data with different orientation of fragments, N(^{2}D) + H_2O, HNO + H, HON + H, NH + OH, H_2 + NO, and O + NH_2. These data were replicated for bond dissociation distances larger than 4 Å up to separation distances of approximately 9 Å.

Data for multireference regions, the open-shell dissociation pathways of intermediates, were calculated using the MS-CASPT2(11e,11o)/cc-pVTZ method. These data specifically involve dissociation pathways of intermediates to make HON + H, NH + OH, and O + NH_2 products. In these regions data for separation of H−N and N−O distances between 2 and 4 Å were calculated using the MS-CASPT2(11e,11o)/cc-pVTZ method. The CASPT2 method gives dissociation energies that differ by roughly 4 kcal mol^{-1} than the more accurate benchmark UCCSD(T) results. Thus, CASPT2 absolute energies were shifted by a constant amount equal to the difference in those energies and the UCCSD(T)-F12/aug-cc-pVTZ ones for the noninteracting products and then added to the data set to be compatible with the data set. Using the constant shift is reasonable because it is used in the near dissociation regions. Roughly 50 000 energy points were calculated for multireferences regions for different orientation of mentioned fragments to describe these regions correctly. Details of these pathways will be explained with properties of the PES in the next section.

FITTING THE POTENTIAL ENERGY SURFACE

The PES is represented by factored polynomials that are invariant with respect to all permutations of like atoms.[17] The variables of these polynomials are all the internuclear distances, transformed to Morse-like variables $y_{i,j} = \exp(-r_{i,j}/\lambda)$, where $r_{i,j}$ are the internuclear distances between atoms i and j and λ is a range parameter, which is typically between 2 and 3 bohr. In the present case it is 2 bohr. The polynomials are restricted to a maximum total order of 6, and this results in 502 linear coefficients, one for each polynomial. Fitting is done by a standard linear least-squares method, with a simple weight for the energies, namely $E_0/(E + E_0)$ for a configuration at energy E, where E_0 is the electronic energy of the global minimum (H_2NO intermediate). The final number of configurations is roughly 312 000 energy points at the UCCSD(T)-F12/aug-cc-pVTZ level of theory. The energies of the data set extend to roughly 300 kcal mol^{-1} above global minimum, H_2NO. The weighted-root-mean-square for the energy points below 120 kcal mol^{-1}, relative to the global minimum, the interest energy range of the present work, is 0.89 kcal mol^{-1}.

PROPERTIES OF THE PES

Figure 1 presents the usual schematic of the multichannel "ZPE-corrected" potential energy surface for the N(^{2}D) + H_2O

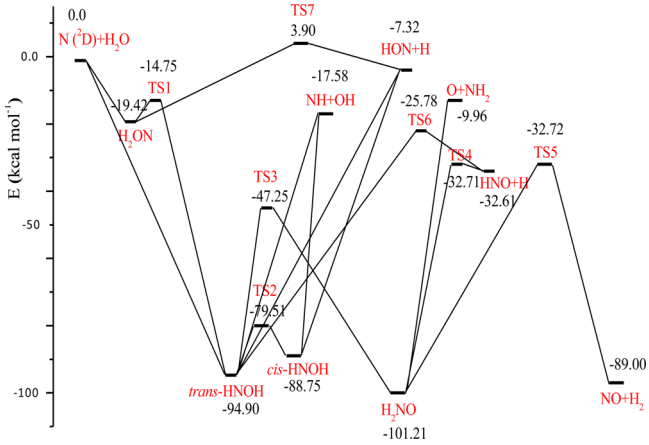

Figure 1. Energy schematic for the fitted PES for the N(^{2}D) + H_2O reaction pathways .

reaction. The energy zero is the reactant energy. The relative energies of stationary points without ZPE at the UCCSD(T)-F12/aug-cc-pVTZ, UCCSD(T)-F12/aug-cc-pVQZ level and the PES are given in Table 1. Ab initio results with harmonic ZPEs for products of reactions are given in parentheses. We also show the experimental values of products calculated from thermodynamics data of ref 21. Figure 2 shows the comparison of stationary point structures obtained from optimization of the PES and optimized geometries at the UCCSD(T)/6-311+G-(d,p) level of theory.

Now we discuses details of potential energy surface calculated at the UCCSD(T)-F12/aug-cc-pVTZ level and the fitted PES as follows: reactants, intermediates, and their isomerization and finally dissociation channels. First we consider the N(^{2}D) and H_2O reactants. Figure 3 shows potential energy curves of three orientations of reactants interactions calculated at the UCCSD(T)-F12/aug-cc-pVTZ level. As seen in Figure 3a, nonplanar insertion of N to oxygen of H_2O leads to the H_2ON intermediate. The association pathway is barrierless, and the intermediate is 20.2 kcal mol^{-1} below the reactants at the UCCSD(T)-F12/aug-cc-pVTZ level. As presented in Figure 3b,c, the N−H interaction of reactants is repulsive for two planar orientations of N and H atoms. As Figure 3 shows, the PES shows good agreement with the ab initio calculations. Via a three-centered transition state (TS1), H_2ON isomerizes to make *trans*-HNOH. TS1 lies 14.1 kcal mol^{-1} below the reactant asymptote at the UCCSD(T)-F12/aug-cc-pVTZ level; this agree well with the 14.7 kcal mol^{-1} value of the PES. Figure 4a shows the good agreement of the fitted PES with CCSD(T) calculations for IRC of the isomerization of H_2ON → *trans*-HNOH. *trans*-HNOH could be generated directly via an H-migration through association of N(^{2}D) and H_2O reactants without passing through H_2ON minimum. There is another possible dissociation channel for the H_2ON intermediate, namely dissociation to HON (^{3}A″) + H products, a process that goes through TS7. The energy of this transition state is 4.5 kcal mol^{-1} above the reactant asymptote at the UCCSD(T)-F12/aug-cc-pVTZ level, in good agreement with the PES saddle points with 3.9 kcal mol^{-1}. The *trans*- and *cis*-HNOH isomerization path connects via a saddle

dx.doi.org/10.1021/jp410935k | J. Phys. Chem. A 2014, 118, 545−553

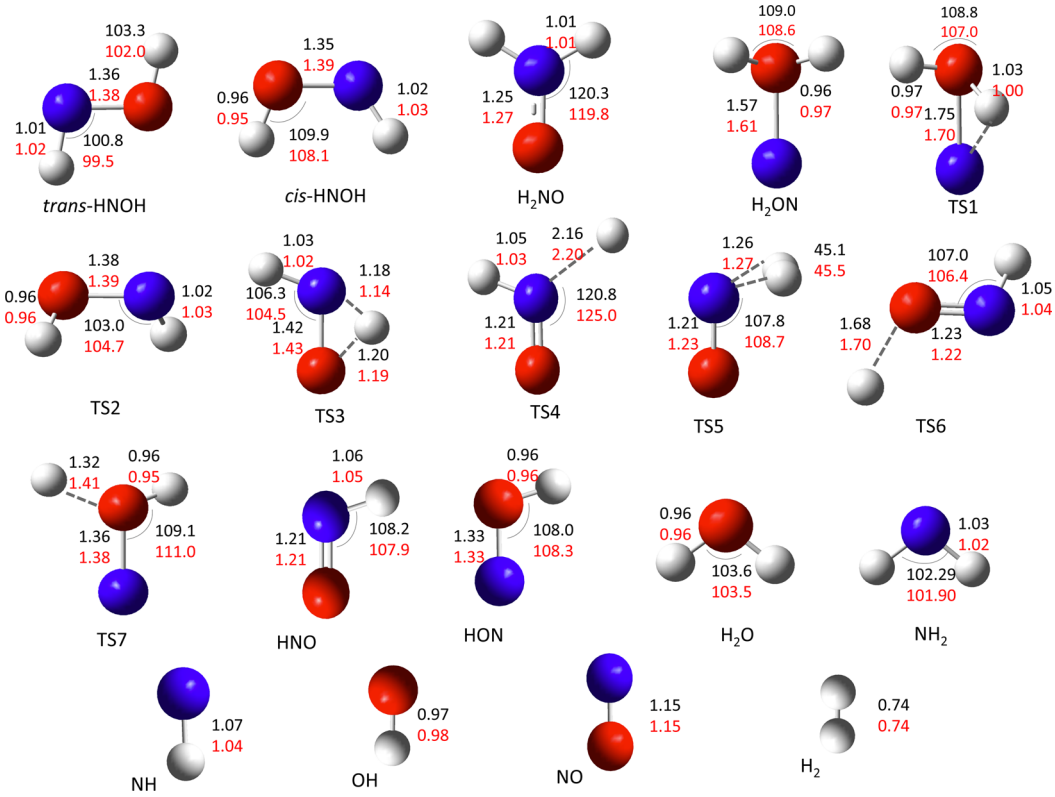

Figure 2. Structures (angstroms and degrees) of stationary points. Optimized geometries parameters at the UCCSD(T)/6-311+G(d,p) level (black) are given followed by PES values (red).

point (TS2). TS2 lies 14.6 kcal mol^{-1} above trans-HNOH at the UCCSD(T)-F12/aug-cc-pVTZ level. The PES describes this path with a 15.4 kcal mol^{-1} barrier.

Next we consider the possible dissociation channels of *trans*- and *cis*-HNOH intermediates. NH and OH fragments can form through simple N−O bond rupture of *trans*- and *cis*-HNOH. The potential energy of these products (R1) is −18 kcal mol^{-1} at the UCCSD(T)-F12/aug-cc-pVQZ level compared with −17.6 kcal mol^{-1}, described by the PES with respect to N(^{2}D) + H_2O reactants. Panels a and b of Figure 5 compare ab initio minimum energy paths of formation of NH + OH through dissociation of *trans*- and *cis*-HNOH intermediates that shows good agreement with the fitted PES.

As shown in Figure 5c,d, N−H bond dissociations of *trans*- and *cis*-HNOH intermediates lead to products of reaction R3. Minimum energy paths for both isomers show good agreement with the MS-CASPT2/cc-pVTZ level calculations. The exothermicity of this reaction is −7.2 kcal mol^{-1} at the UCCSD(T)-F12/aug-cc-pVTZ level, −7.2 kcal mol^{-1} at the UCCSD(T)-F12/aug-cc-pVQZ level, and −7.3 kcal mol^{-1} by the PES.

The global minimum of this system is H_2NO. A path that proceeds via a three-centered transition state, TS3, for hydrogen migration of *trans*-HNOH leads to this intermediate. The energy of this saddle point is −47.4 kcal mol^{-1} at the UCCSD(T)-F12/aug-cc-pVTZ level with respect to reactants in comparison to −47.3 kcal mol^{-1} in the PES. Agreement of the ab initio IRC of this isomerization path with the PES is shown in Figure 4b. Reaction R2, production of HNO(1A″) + H, could proceed through two channels. The first one is N−H bond rupture of H_2NO via TS4. The NH bond length at the saddle point is 2.16 Å, which agrees with the Sumathi et al.[11] result of 2.16 Å. This is in contrast to the optimized value of ref 12 at the MP2(full)/cc-pVTZ level. TS4 lies 2.7 kcal mol^{-1} at the UCCSD(T)-F12/aug-cc-pVTZ level (including ZPE) above the HNO(1A″) + H asymptote, compared with 6.2 kcal mol^{-1} reported in ref 12.

The second channel that can generate HNO(1A″) + H products is dissociation of *trans*-HNOH. That path proceeds through TS6 with an energy of −25.5 kcal mol^{-1} at the UCCSD(T)-F12/aug-cc-pVTZ level relative to the reactants asymptote where again very good agreement is seen with the PES.

Production of H_2 + NO, reaction R4, is the most exothermic channel with −89.1 kcal mol^{-1} energy at the UCCSD(T)-F12/aug-cc-pVQZ level. According to the schematic in Figure 1, H_2NO dissociates to H_2 + NO via TS5 with a 68.5 kcal mol^{-1} barrier according to the PES. Figure 3c compares ab initio and the PES calculations of the relevant IRC. The IRC of this pathway was examined using the MS-CASPT2(11e,11o)/cc-pVTZ method. The ground-state dissociation path for this pathway is in agreement with the results in refs 11 and 13.

Finally, the last reaction is reaction R5 where reactants produce $NH_2(^2B_1)$ + O(^{3}P) fragments. This channel could take place through N−O bond dissociation of H_2NO. Again, the exothermicities of this reaction at the UCCSD(T)-F12 level with both the aug-cc-pVTZ and aug-cc-pVQZ basis set and the fitted PES show good agreement, as presented in Table 1.

Next we consider the quasiclassical trajectory (QCT) calculations of the N + H_2O and N + D_2O to NH(D) + OH(D) reactions, reaction R1.

dx.doi.org/10.1021/jp410935k | J. Phys. Chem. A 2014, 118, 545−553

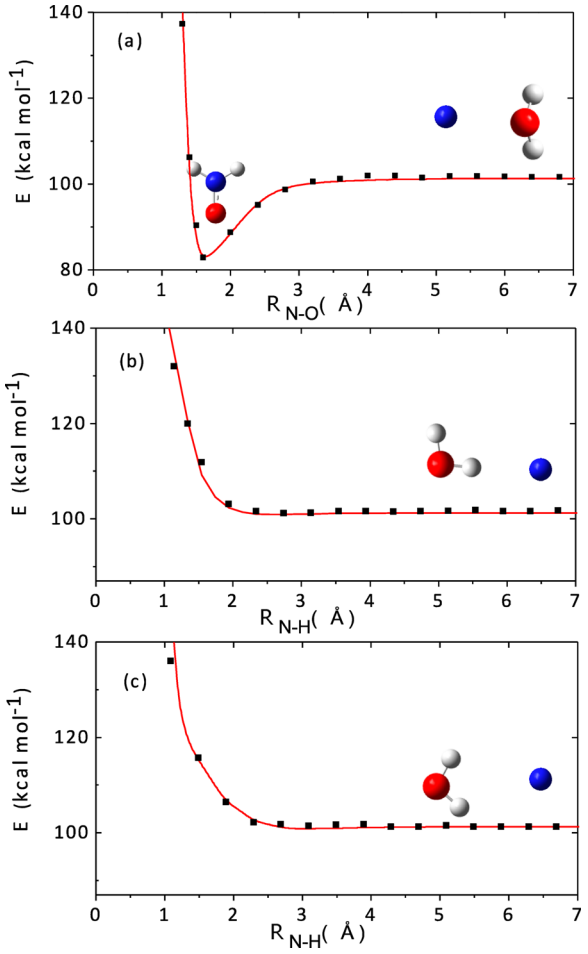

Figure 3. Potential energy curves of H_2O---N as a function of N−O and N−H distances at three different orientations, formation of H_2ON at the UCCSD(T)-F12/aug-cc-pVTZ//UMP2/6-311+G(d,p) level (a) and repulsive potential of N−H interaction for two different orientations (b, c) calculated at the UCCSD(T)-F12/aug-cc-pVTZ level. Black squares are data from the PES and red curves are ab initio data.

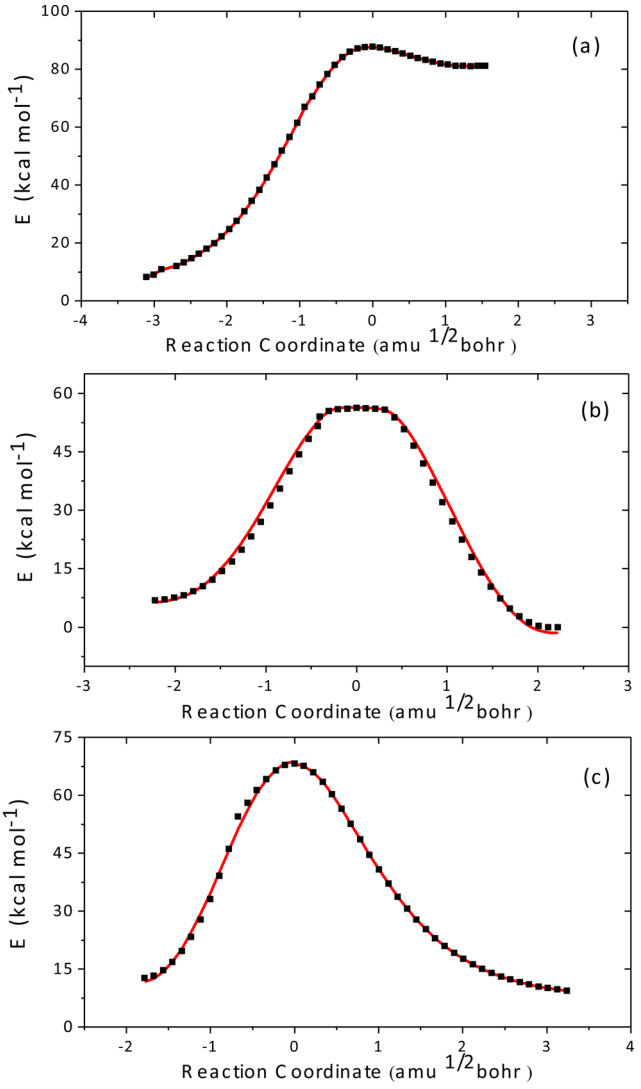

Figure 4. IRC for TS1 (a), TS3 (b), and TS4 (c), calculated at the UCCSD(T)-F12/aug-cc-pVTZ//UMP2/6-311+G(d,p) level (black squares) and compared with the PES (red curves).

QUASICLASSICAL TRAJECTORY CALCULATIONS

$N(^2D) + H_2O$ Reaction. The QCT calculations of the $N(^2D) + H_2O$ reaction were performed using the global fitted PES. Standard normal-mode sampling[18] of the zero-point phase space of H_2O was done with zero angular momentum. The initial distance between N and H_2O is 15 bohr. The relative orientation of the reactants was randomly sampled. The impact parameter (b) was scanned between 0 and 7 bohr with a step size of 0.5 bohr.

The QCT calculations were performed at a collision energy (E_{coll}) of 1.5 kcal mol^{-1}. This energy corresponds to the energy of experiment of Umemoto and co-workers.[7] The trajectories were propagated with the time step of 0.12 fs for a maximum of 500 000 time steps. This reaction produces several products through different mechanisms that correspond to different lifetimes of intermediates. So for some products this number of time steps is not necessary. The trajectories were terminated when one of the internuclear distances became larger than 20 bohr. A total of 52 500 trajectories, 3500 trajectories for each b, were run. Products of all reactions R1−R5 have been observed, but the present work reports the detailed results of reaction R1. The energy available to the products NH + OH is 32.9 kcal mol^{-1}. This value is the sum of the ZPE (from the PES) of H_2O plus the exoergicity of 17.6 kcal mol^{-1} (from the PES) plus the initial collision energy of 1.5 kcal mol^{-1}.

Figure 6 shows a representation of two sample trajectories leading to the products through different mechanisms. In the first trajectory, collision of reactants directly makes HNOH in contrast with the second one where production of H_2ON is observed. Next, the HNOH intermediate dissociates to NH + OH. As seen, the trajectory with the longer lifetime of HNOH leads to products with less vibrational energy of products.

Now we discuss details of the calculation of the final-state distributions of NH and OH products. Harmonic wavenumbers of NH and OH are 3158 and 3645 cm^{-1} according to the fitted PES. So the first harmonic vibrational states of NH and OH have 13.5 and 15.6 kcal mol^{-1} energy, respectively.

Specifically, our goal is to obtain final quantized rotational and vibrational distribution of each product summed over the rovibrational distributions. The rotational quantum numbers have been assigned for products as follows. The classical angular momentum j of OH and NH was calculated using the final Cartesian coordinates and velocities. The quantum

dx.doi.org/10.1021/jp410935k | J. Phys. Chem. A 2014, 118, 545−553

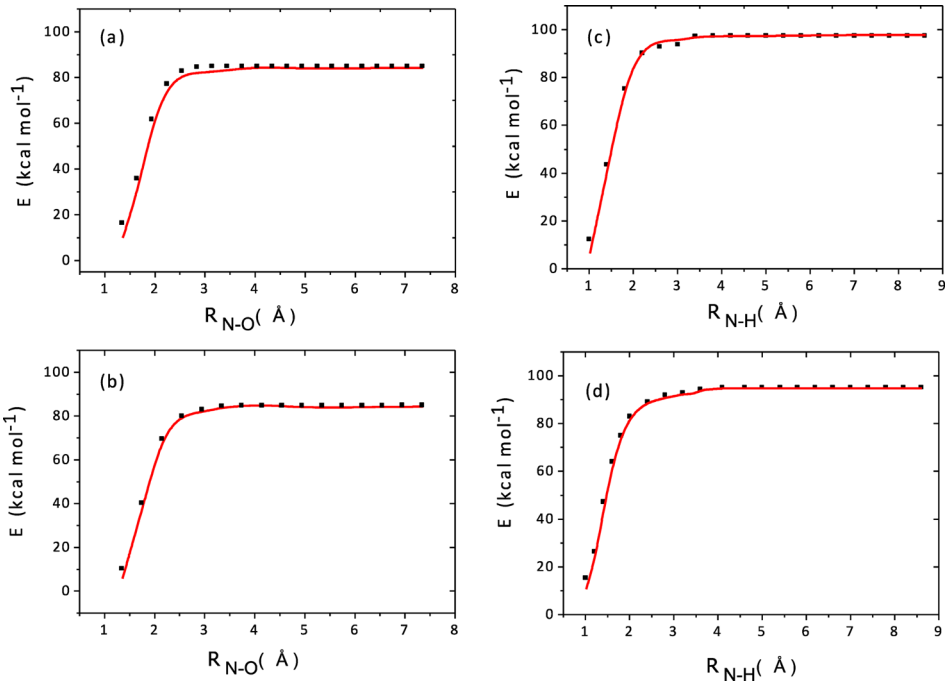

Figure 5. *cis*- (a) and *trans*-HNOH (b) dissociation pathways to NH + OH products. *trans*- (c) and *cis*-HNOH (d) dissociation pathways to HON + H products. The red curves are from the PES, and black squares are scaled at the MS-CASPT2(11e,11o)/cc-pVTZ level relative to separated fragments' energies at the CCSD(T)/aug-cc-pVTZ level. These paths were constructed using CASPT2 calculations for bond distances between 2 and 4 Å and CCSD(T) fragments data for bond distances longer than 4 Å.

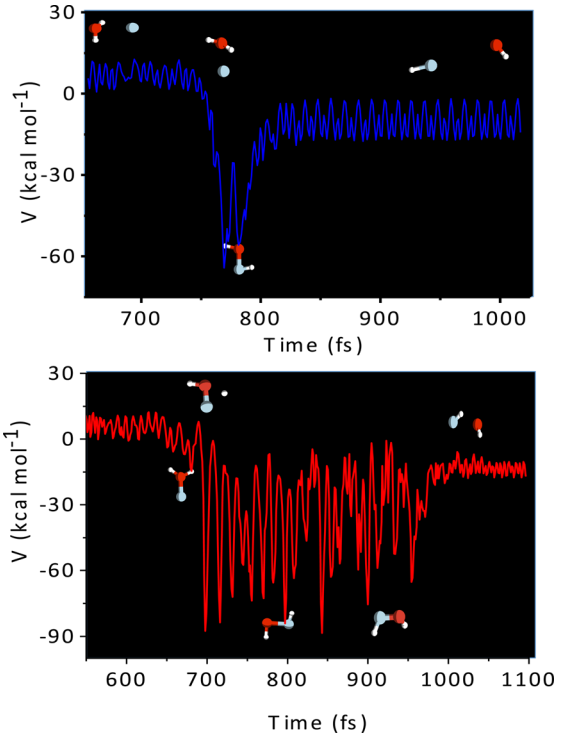

Figure 6. Potential energy of two sample trajectories leading to reaction R1. The first trajectory makes HNOH directly; the second one passes through H_2ON and TS1.

number J was calculated from the quantum mechanical expression $j = (J(J + 1))^{1/2}$ by rounding J to the nearest integer value.

For the vibrational distributions standard histogram binning (HB) was done. That is, the classical vibrational actions were rounded to the nearest integers. In addition, Gaussian binning (GB)[19,20] was done. This approach deals effectively with the quantization of vibrational energies and the well-known zero-point violation issue in histogram binning. The most rigorous way to apply GB is to obtain the correlated vibrational distribution. This is obtained by first computing the product of the GB weight for each product, OH and NH, for the trajectory p. This product is given by $G_p(n_{OH})\, G_p(n_{NH})$, where $G_p(n)$ is given by

$$G_p(n) = \frac{\beta}{\sqrt{\pi}} \exp(-\beta^{2[(E(n_p')-E(n))/2E(0)]^2}) \quad (1)$$

In this equation $\beta = 2(\ln 2)^{1/2}/\delta$ and δ is the full-width at half-maximum. $E(n)$ is the harmonic vibrational energy of mode n, $E(0)$ is the harmonic zero-point energy, and $E(n_p')$ is the vibrational energy of trajectory p. The harmonic energies of OH and NH are similar so the same β-parameter was used for both weights. In terms of this correlated weight the desired normalized distribution for each product summed over the vibrational distribution of the other product is given by, for example for state n of OH (n_{OH}),

$$P_{GB}(n_{OH}) = \frac{\sum_p^{N(n_{OH})} \sum_{n_{NH}} G_p(n_{OH})\, G_p(n_{NH})}{\sum_{n_{OH}} \sum_p^{N(n_{OH})} \sum_{n_{NH}} G_p(n_{OH})\, G_p(n_{NH})} \quad (2)$$

where the sum over n_{NH} is the sum over all states of second fragments, here NH, and the sum over p is simply the sum over all trajectories leading to the products. Finally, to specify the weight, a value of β needs to be determined. The general condition is that for a given integer value of n, the Gaussian weight should have a very small value at adjacent quantum numbers. In the present case a value of 11 was chosen for β. This gives a weight that is essentially zero for vibrational energies halfway between harmonic quantum energies.

dx.doi.org/10.1021/jp410935k | J. Phys. Chem. A 2014, 118, 545−553

Figure 7 presents the classical vibrational distribution of OH. As seen, a considerable fraction of products have vibrational

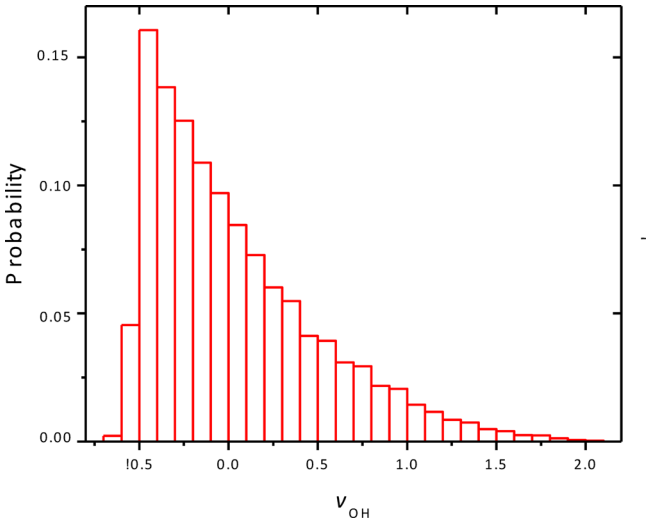

Figure 7. Distribution of the classical vibrational action number of OH.

energies below ZPE. So ZPE violation of one fragment could release an incorrect amount of energy into the other fragment. Table 2 presents populations of the vibrational state using both

Table 2. Vibrational-State Population of NH and OH Products Using QCT-HB and QCT-CGB and Average of Rotational Energy (E_r, kcal mol^{-1}) for the Indicated States of Products[a]

		HB	CGB	EXP[b]
NH(v=1)/NH(v=0)		0.36	0.32	0.3
OH(v=1)/OH(v=0)		0.2	0.17	0.05
	$E_r(v=0)$		$E_r(v=1)$	$E_r(v=2)$
	QCT	exp[b]	QCT	exp[b]	QCT
NH	5.20	4.59	4.17	2.58	
OH	3.90	3.80	3.46		
ND	5.46		4.80		2.98
OD	3.79		3.49		2.25

[a]HB and CGB are acronyms for histogram binning and correlated Gaussian binning, as explained in the text. [b]Reference 7.

binning methods. The ratio of NH(v=1)/NH(v=0) was determined to be 0.32 using CGB and 0.36 using HB. The OH(v=1)/OH(v=0) ratio was calculated to be 0.2 and 0.17 using HB and CGB approaches.

Next we calculate the Boltzmann rotational distribution for products that are described by the equation $P(J) = (2J + 1)\exp[-E_{int}(J)/kT_{rot.}]$. So, for the ground vibrational state ($v = 0$) of NH, the logarithm of the population densities for the different rotational levels $P(J)/(2J + 1)$ is plotted against internal energy (E_{int}) and the result is shown in Figure 8. The rotational temperature for NH(v=0) products is reported to be 3000 K by experiment.[7] We plotted the Boltzmann curve of the rotational temperature of 3000 K for the NH product as well, which shows agreement with our results. The same Boltzmann plot of the relative population of OH(v=0) is presented in Figure 9. Again, the reported 2000 K rotational temperature has been plotted. The average of vibrational energies of fragments

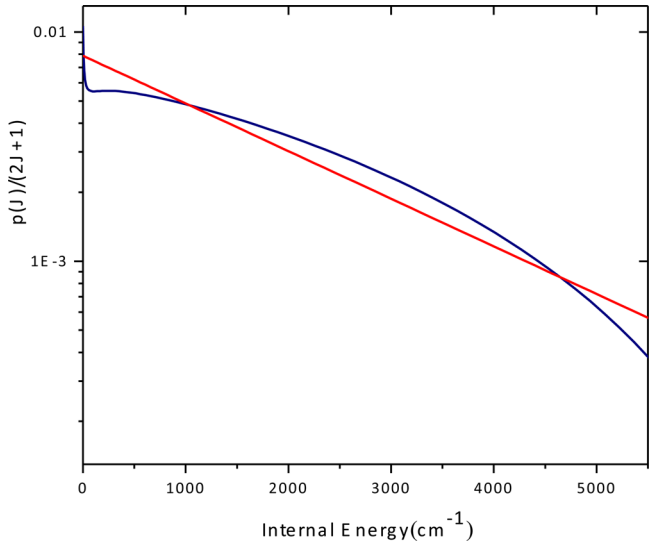

Figure 8. Rotational-state distribution of NH($^3\Sigma$,v=0) product (blue) and Boltzmann plot at 3000 K (red).

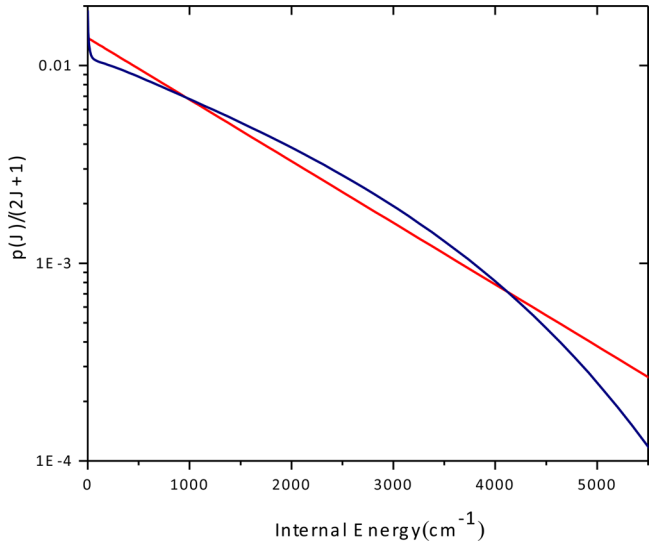

Figure 9. Rotational-state distribution of OH($^2\Pi$,v=0) product (blue) and Boltzmann plot at 2000 K (red).

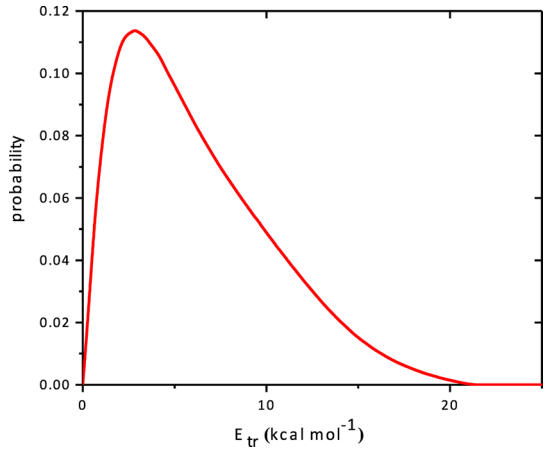

Figure 10. Translational energy distribution of NH + OH products.

dx.doi.org/10.1021/jp410935k | J. Phys. Chem. A 2014, 118, 545−553

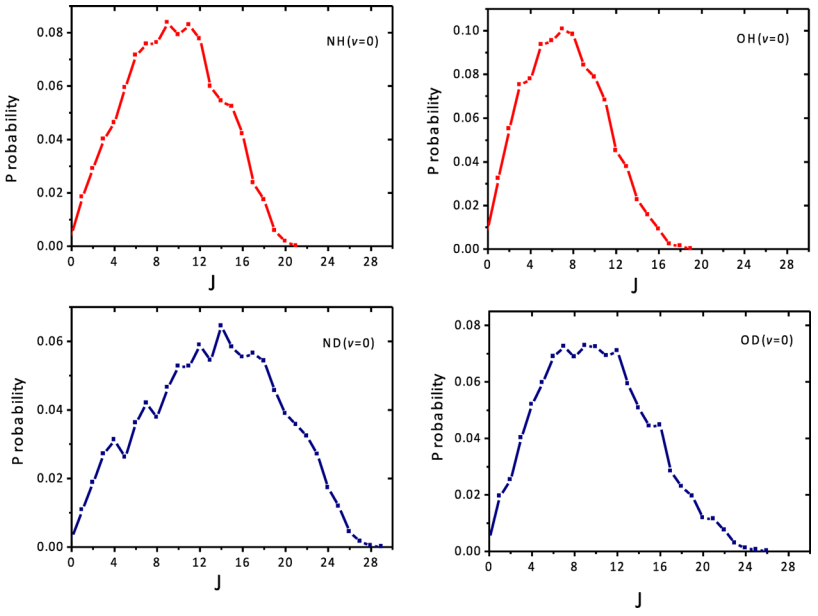

Figure 11. Calculated normalized rotational population of products of $N(^2D) + H_2O$ and $N(^2D) + D_2O$ reactions.

for two vibrational states and comparison with the values of ref 7 are given in Table 2, which shows good agreement.

Finally, the translational energy distribution of reaction R1 is represented in Figure 10. Here we adopt the "soft constraint" in which trajectories are discarded if products are formed with less than the sum of the (harmonic) ZPEs of each fragment. The figure shows a peak at about 4.5 kcal mol^{-1} and the average of translational energy distribution is 6.3 kcal mol^{-1}.

$N(^2D) + D_2O$ Reaction. Using the global fitted PES, the QCT calculations of the $N(^2D) + D_2O$ reaction were investigated as well. The calculations for this reaction were performed with the same initial conditions of the $N(^2D) + H_2O$ reaction. Again a total of 52 500 trajectories with 1.5 kcal mol^{-1} collision energy were run. Here we consider details of energy distribution of ND + OD products and comparison with NH + OH.

With the same approach explained in the previous section, the vibrational level populations of ND and OD have been investigated. According to the PES, the harmonic wave numbers of ND and OD are 2235 and 2695 cm^{-1}, which makes the second harmonic state of fragments available. The populations of vibrational states of ND(v=0,1,2) are 0.62, 0.28, and 0.1 using HB in comparison with CGB values, 0.63, 0.27, and 0.1. Again the OD fragment shows less vibrational excitation in comparison with OD. Using the CGB method OD(v=0,1,2) is calculated as 0.77, 0.19, 0.03 and 0.76, 0.20, 0.03 using HB. ND(v=0)/ND(v=1) = 0.4 and OD(v=0)/OD(v=1) = 0.05 are reported by ref 7. For ND(v=2) and OD(v=2) there are no data available.

Rotational quantum number distributions and rotational energies of ND and OD are calculated as well. Rotational energies of fragments are presented in Table 2. As seen, vibrational energies of products of both reactions are similar. Umemoto and co-workers[7] reported the same rotational temperature for products of the $N(^2D) + H_2O$ and $N(^2D) + D_2O$ reactions. Here we compare distributions of rotational quantum number of isomer products. Figure 11 presents rotational population of products. The J-distribution of NH(v=0) peaks around 10 compared with 14 for ND(v=0). For OH(v=0) and OD(v=0), the product maxima of the J-distributions are about 7 and 9. We also calculated the translational energy distribution for this reaction. The average of translational energy distribution of ND + OD corresponds to 6.3 kcal mol^{-1}.

As seen, for products of both reactions, nonstatistical energy distributions have been observed both rotationally and vibrationally, which could be explained by the short-lived time of the intermediates. More details of the mechanism of this reaction will be considered in the future along with reactions that could make the H atom.

SUMMARY AND CONCLUSIONS

We reported a global potential energy surface for the $N(^2D) + H_2O$ reaction . The PES is a permutationally invariant precise fit to roughly 312 000 electronic energies mostly at the UCCSD(T)-F12/aug-cc-pVQZ level of theory supplemented with some MS-CASSPT2 calculations. The PES reproduces five exit channels of the title reaction accurately. The PES accurately describes stationary points and minimum energy paths for product channels. Quasiclassical trajectory calculations were performed using the fitted PES for the $N(^2D) + H_2O$ and $N(^2D) + D_2O$ reactions. The product energy distribution of reaction R1, OH (OD) + NH(ND), has been investigated at 1.5 kcal mol^{-1} collision energy. NH and OH products both are rotationally excited, in agreement with experiment. Nonstatistical energy distribution of products shows good agreement with experiment.

AUTHOR INFORMATION

Corresponding Authors

*Z. Homayoon: e-mail, zhomayo@emory.edu.
*J. M. Bowman: e-mail, jmbowma@emory.edu.

Notes

The authors declare no competing financial interest.

ACKNOWLEDGMENTS

Discussions with Dr. Francesco Evangelista are gratefully acknowledged.

We thank the Army Research Office (W911NF-11-1-0477) for financial support.

REFERENCES

(1) Bozzelli, J. W.; Dean, A. M. In *Gas-phase Combustion Chemistry*, 2nd ed.; Gardiner, W. C., Jr., Ed.; Springer-Verlag: New York, 2000; Chapter 2.

(2) Diau, E. W.; Halbgewachs, M. J.; Smith, A. R.; Lin, M. C. Thermal reduction of NO by H_2: Kinetic measurement and computer modeling of the HNO + NO reaction, Int. *J. Chem. Kinet.* **1995**, *27*, 867−881.

(3) Soto, M. R.; Page, M. J. *Ab initio* variational transition-state-theory reaction-rate calculations for the gas-phase reaction H+HNO→ H_2+NO. *J. Chem. Phys.* **1992**, *97*, 7287−7296.

(4) Adamson, J. D.; Farhat, S. K.; Morter, C. L.; Glass, G. P.; Curl, R. F.; Phillips, L. F. The Reaction of NH_2 with O. *J. Phys. Chem.* **1994**, *98*, 5665−5669.

(5) Misra, D. P.; Sanders, D. G.; Dagdigian, P. J. Internal state distribution of OD produced from the $O(^3P)$ + ND_2 reaction. *J. Chem. Phys.* **1991**, *95*, 955−962.

(6) Misra, D. P.; Dagdigian, P. J. Dynamics of the $O(^3P)$+NH_2 reaction: the HNO + H product channel. *Chem. Phys. Lett.* **1991**, *185*, 387−392.

(7) Umemoto, H.; Asai, T.; Hashimoto, H.; Nakae, T. Reactions of $N(^2D)$ with H_2O and D_2O; Identification of the Two Exit Channels, NH(ND)+ OH(OD) and H(D) + HNO(DNO). *J. Phys. Chem. A* **1999**, *103*, 700−704.

(8) Casavecchia, p.; Balucani, N.; Cartechini, L.; Capozza, G.; Bergeat, A.; Volpi, C. G. Crossed beam studies of elementary reactions of N and C atoms and CN radicals of importance in combustion. *Faraday Discuss.* **2001**, *119*, 27−49.

(9) Yang, D. L.; Koszykowski, M. L.; Durant, J. L., Jr. The reaction of NH_2 (X^2B_1) with O (X^3P): A theoretical study employing Gaussian 2 theory. *J. Chem. Phys.* **1994**, *101*, 1361−1368.

(10) Duan, X.; Page, M. *Ab initio* variational transition state theory calculations for the O+NH_2 hydrogen abstraction reaction on the $^4A'$ and $^4A''$ potential energy surfaces. *J. Chem. Phys.* **1995**, *102*, 6121−6127.

(11) Sumathi, R.; Sengupta, D.; Nguyen, M. T. Theoretical Study of the H_2 + NO and Related Reactions of $[H_2NO]$ Isomers. *J. Phys. Chem. A* **1998**, *102*, 3175−3183.

(12) Kurosaki, Y.; Takayanagi, T. *Ab Initio* Molecular Orbital Study of the $N(^2D)$ + H_2O Reaction. *J. Phys. Chem. A* **1999**, *103*, 436−442.

(13) Kurosaki, Y.; Takayanagi, T. *Ab initio* molecular orbital study of potential energy surface for the $H_2NO(^2B_1)$→$NO(^2\Pi)$+H_2 reaction. *J. Mol. Struct. (THEOCHEM)* **2000**, *507*, 119−126.

(14) Werner H. J.; Knizia G.; Mandy F. R.; Schütz M.; Celani P.; Korona T.; Lindh R.; Mitrushenkov A.; Rauhut G.; Shamasundar K. 461 R.; et al. *MOLPRO*, version 2008; http://www.molpro.net.

(15) Frisch, M. J.; Trucks, G. W.; Schlegel, H. B.; Scuseria, G. E.; 463 Robb, M. A.; Cheeseman, J. R .; Scalmani, G.; Barone, V.; Mennucci, 464 B.; Petersson, G. A.; et al. *GAUSSIAN 09*, Revision A02; Gaussian, Inc.: Wallingford, CT, 2009.

(16) Karlstr€om, G.; Lindh, R.; Malmqvist, P.-Å.; Roos, B. O.; Veryazov, V.; Widmark, P.-O.; Cossi, M.; Schimmelpfennig, B.; Neogrady, P.; Seijo, L. MOLCAS: A Program Package for Computational Chemistry. *Comput. Mater. Sci.* **2003**, *28*, 222−239.

(17) Braams, B. J.; Bowman, J. M. Permutationally Invariant Potential Energy Surfaces in High Dimensionality. *Int. Rev. Phys. Chem.* **2009**, *28*, 577−606.

(18) Hase, W. L. Classical Trajectory Simulations: Initial Conditions. In *Encyclopedia of Computational Chemistry*; Allinger, N. L., Eds.; Wiley: New York, 1998; Vol. *1*, pp 402−407.

(19) Bonnet, L. Classical dynamics of chemical reactions in a quantum spirit. *Int. Rev. Phys. Chem.* **2013**, *32*, 171−228.

(20) Czako, G.; Bowman, J. M. Quasiclassical trajectory calculations of correlated product distributions for the F+CHD_3(v_1 = 0,1) reactions using an *ab initio* potential energy surface. *J. Chem. Phys.* **2009**, *131*, 244302−244320.

(21) Afeefy, H. Y.; Liebman, J. F.; Stein, S. E. Neutral Thermochemical Data. In *NIST Chemistry WebBook*; Linstrom, P.J., Mallard, W.G., Eds.; NIST Standard Reference Database Number 69; National Institute of Standards and Technology: Gaithersburg, MD, http://webbook.nist.gov (retrieved November 3, 2013).